

Two-photon absorption-induced self-phase modulation in GaAs–AlGaAs waveguides for surface-emitted second-harmonic generation

Todd G. Ulmer, Ronson K. Tan,* Zhiping Zhou, Stephen E. Ralph, Richard P. Kenan, and Carl M. Verber

School of Electrical and Computer Engineering, Georgia Institute of Technology, Atlanta, Georgia 30332-0250

Anthony J. SpringThorpe

Nortel Advanced Technology Laboratory, Ottawa, Ontario K1Y 4 H7, Canada

Received November 24, 1998

Performance-limiting asymmetric distortion is observed in the spectra of fundamental pulses transmitted through GaAs–Al_{0.9}Ga_{0.1}As multilayer waveguides designed for surface-emitted second-harmonic generation. This behavior is attributed to refractive-index changes resulting from the accumulation of free carriers created by two-photon absorption in the GaAs layers. Numerical simulations of the intensity-dependent spectra by use of the separately measured two-photon absorption coefficient are shown to be in good agreement with the observed spectra. © 1999 Optical Society of America

OCIS codes: 230.4320, 190.4180, 190.4160.

For high-intensity pulses in semiconductor waveguides, two-photon absorption (TPA) can become significant not only as a loss mechanism but also as a source of carrier-induced refractive-index changes. The resulting asymmetric distortion of the pulse spectrum through self-phase modulation can be more detrimental in certain applications than the loss associated with TPA alone. One example is surface-emitted second-harmonic generation¹ (SESHG) in quasi-phase-matched (QPM) waveguides, which exploits the large $\chi^{(2)}$ of semiconductors and the relative ease of producing QPM vertical layers by use of conventional epitaxy techniques. Owing to the limited interaction length associated with counterpropagating short pulses in the surface-emitted geometry, conversion efficiencies are typically low, and large input intensities are needed for useful SESHG powers. If the intensity is large enough for significant TPA, the associated carrier-induced spectral distortion can negatively affect wavelength-dependent SESHG device applications, such as integrated optical spectrometers.^{2,3} Furthermore, SESHG correlators⁴ and temporal demultiplexers⁵ are also penalized by the associated temporal distortion. Here we present results from a SESHG experiment in which the fundamental spectrum is distorted asymmetrically, and we demonstrate by simulation that this distortion can result from refractive-index changes caused by TPA-generated carriers. The separately measured TPA coefficient in the QPM waveguide is consistent with the self-phase modulation needed to produce the observed distortion.

The waveguide is designed for operation near $\lambda_{\text{fund}} \approx 1.5 \mu\text{m}$, with a multilayer core consisting of six half-wavelength layers of GaAs [high $\chi^{(2)}$] alternating with five layers of Al_{0.9}Ga_{0.1}As [low $\chi^{(2)}$] so that a QPM condition is achieved.^{1,6} The upper and lower Al_{0.9}Ga_{0.1}As cladding layers are 1.66 and 1.73 μm

thick, respectively, with a 10-nm GaAs cap and a six-period AlAs–GaAs distributed Bragg reflector below. The distributed Bragg reflector reflects the downward-propagating portion of the second harmonic back toward the surface, where it can be collected. The entire structure was grown by molecular beam epitaxy on (100)-oriented semi-insulating GaAs. Channel waveguides were formed by reactive-ion etching 3- μm -wide ribs to a depth of 2.4 μm .

For all the data reported here the fundamental wavelength was near 1.50 μm and the FWHM pulse width was 240 fs. The polarization state was controlled with a half-wave plate, and the power was adjusted with a variable attenuator. The fundamental pulse transmitted through the waveguide was collected with a standard single-mode fiber and measured with an optical spectrum analyzer. Similarly, the SESHG that was generated by the fundamental pulse was collected with a 100- μm -core multimode fiber positioned above the waveguide. We readily obtained the counterpropagating geometry by allowing the fundamental pulse to reflect through itself at the rear waveguide facet.

Since the fundamental photon energy is greater than one-half the bandgap of GaAs, TPA can occur. The presence of TPA was verified by separate waveguide transmission measurements, which also provided the TPA coefficient. Furthermore, the recombination of TPA-generated free electron–hole pairs was observed as band-edge luminescence, as shown in Fig. 1. The time-averaged band-edge luminescence was collected above the input facet, where the peak intensity and TPA are highest. The peak emission wavelength shifted by less than 5 MeV, from 872 nm at 4 GW/cm² to 875 nm at 20 GW/cm², showing that thermal effects that may be present are not large. The slope of the high-energy luminescence also confirms the absence of significant heating. The linear polarization of the input fundamental was oriented at

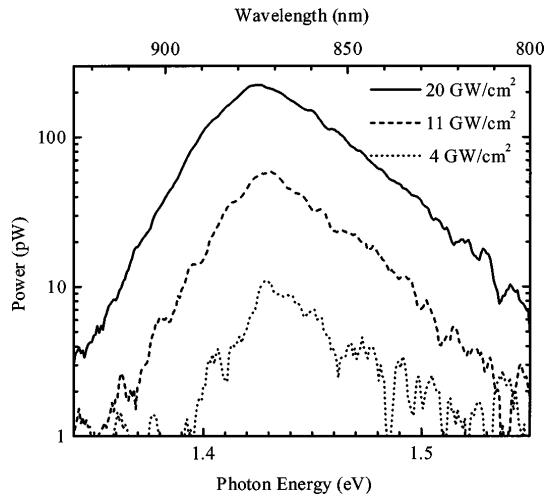


Fig. 1. Room-temperature band-edge luminescence resulting from the subbandgap fundamental ($\lambda \sim 1.5 \mu\text{m}$), measured above the input facet of the waveguide. The intensity dependence confirms that carrier generation is dominated by TPA. The peak emission wavelength and the high-energy tail verify minimal heating.

45° from vertical, equally exciting both the TE and the TM modes as required for SESHG in (100)-oriented (Al)GaAs.⁷ For pure TE or TM excitation we observed polarization dependence in the TPA, with the TE-polarized fundamental producing as much as double the luminescence intensity of the TM. We observed a similar dependence in the effective TPA coefficient β , which was determined to be 8 cm/GW for the TE mode and 3 cm/GW for the TM mode in a separate nonlinear transmission experiment. The effective β that was used here incorporates the overlap of the mode with the multilayer waveguide core. We note that this dependence is in agreement with that observed previously in bulk AlGaAs waveguides.⁸

Spectral and temporal distortions resulting from free-carrier-induced changes in the refractive index are both instantaneous and potentially long lived. In contrast with previous work,^{9–11} we focus on the spectral distortions related to carriers produced by TPA. Here, TPA-generated carriers created by the first portion of the pulse reduce the index that is experienced by the remainder of the pulse. Thus, when the free-carrier density changes during the time of the pulse, both temporal and spectral asymmetries result. These asymmetric spectral distortions are apparent in Fig. 2(a), in which the observed spectra are shown for the transmitted TE and TM fundamentals. The spectra are increasingly distorted and blueshifted for increasing peak intensities. This asymmetric spectral distortion and eventual splitting at high power are characteristic of carrier-induced self-phase modulation.⁹ In contrast, symmetric spectral distortion is observed for self-phase-modulation related to instantaneous processes, such as the Kerr effect, that are not cumulative. The asymmetric spectral distortion that was observed here requires a cumulative effect, such as a time-dependent carrier density related to the total time-integrated absorption.

We model the evolution of the fundamental complex electric field in the waveguide by coupling the spatial dependence of the electric field with the time dependence of the carrier density^{9,11}:

$$\frac{da}{dz} = -\frac{\alpha}{2}a - \frac{\beta I_{\text{max}}}{2}|a|^2a + ik_0(\sigma_n N + n_2 I_{\text{max}}|a|^2)a, \quad (1)$$

$$\frac{dN}{dt} = -\frac{N}{\tau} + \frac{\beta}{2\hbar\omega} I_{\text{max}}^2 |a|^4. \quad (2)$$

Here, $a = E/\sqrt{I_{\text{max}}}$, α is the linear propagation loss, I_{max} is the peak intensity, k_0 is the free-space wave number, N is the carrier density, n_2 is the bulk nonlinear index, and τ is the carrier lifetime. Time is measured in a reference frame propagating with the pulse. Linear absorption is dominated by light scattering out of the guide, and thus carriers are produced only through TPA. The refractive-index change per carrier pair density, σ_n , is estimated with^{12,13}

$$\sigma_n = -\frac{q^2}{2\omega^2 \epsilon_0 n_0 m_{\text{eff}}} \frac{E_g^2}{E_g^2 - (\hbar\omega)^2}, \quad (3)$$

where m_{eff} is the reduced effective mass. The frequency dependence of σ_n is negligible since the fundamental is far from resonance. Using $n_0 = 3.37$, we find that $\sigma_n = -7.4 \times 10^{-21} \text{ cm}^3$. Equations (1) and (2) were solved numerically for our 1.28-mm guide with $\alpha = 15 \text{ cm}^{-1}$, $\lambda = 1.5 \mu\text{m}$, and $\tau = 1 \text{ ns}$. A Gaussian input pulse with $\tau_{\text{FWHM}} = 240 \text{ fs}$ was

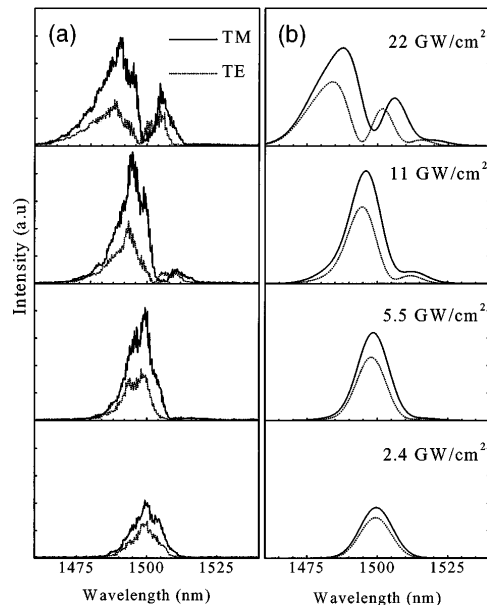


Fig. 2. (a) Transmitted TM and TE fundamental spectra for $1.5\text{-}\mu\text{m}$ excitation at various peak intensities inside the waveguide. (b) Corresponding simulation results, with $\beta^{\text{TM}} = 3 \text{ cm/GW}$, $\beta^{\text{TE}} = 8 \text{ cm/GW}$, and $n_2 = 8 \times 10^{-14} \text{ cm}^2/\text{W}$.

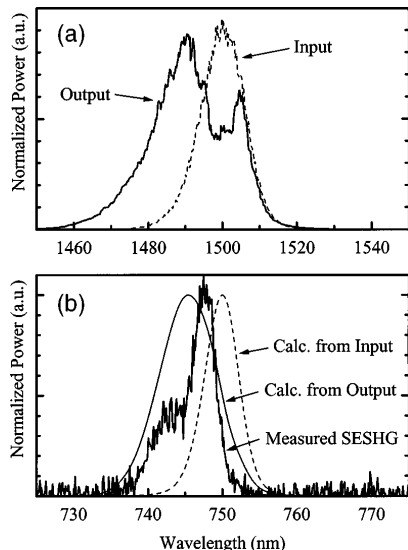


Fig. 3. (a) Normalized fundamental spectra showing asymmetric distortion for 22-GW/cm² peak intensity oriented to excite both the TE and TM modes. (b) Corresponding calculated and measured SESHG spectra. Note that the SESHG would be centered at 750 nm for an undistorted 1.5- μ m fundamental.

assumed. Thus, only the effective nonlinear index n_2 and a fixed coupling efficiency into the guide were adjustable parameters. The numerical simulation produced the temporal behavior of the transmitted pulse, and the power spectrum was then obtained by a Fourier transform.

The calculated spectra for increasing input intensities are shown in Fig. 2(b). The consistent agreement with the observed data in Fig. 2(a) was achieved by use of $n_2 = 8 \times 10^{-14}$ cm²/W for all spectra. With all other parameters fixed, the relative intensity of the transmitted fundamental scales the same as do the observed data. Furthermore, the simulation clearly shows the experimentally observed blueshifts and asymmetric, multi-peaked behavior at higher intensities. We note that the n_2 used in the simulation is smaller than that typically reported for GaAs.⁸ This is expected since the waveguide is a GaAs-Al_{0.9}Ga_{0.1}As layered structure. The fact that the spectra observed for four different input intensities are all well simulated with fixed parameters validates the model and shows that the observations are consistent with the TPA mechanism.

A representative SESHG spectrum and the corresponding fundamental are shown in Fig. 3. The data were observed for a peak fundamental intensity of 22 GW/cm² with the input polarization at 45°, corresponding to a peak carrier density of 8×10^{17} cm⁻³. The calculated SESHG spectra in Fig. 3(b) are obtained from the fundamental spectra in Fig. 3(a) with

$$\mathbf{P}_{\text{NL}}^{(2)}(\omega) = \epsilon_0 \int_{-\infty}^{\infty} \int_{-\infty}^{\infty} \chi^{(2)}(-\omega_{\sigma}; \omega_1, \omega_2) \times \mathbf{E}(\omega_1)\mathbf{E}(\omega_2)\delta(\omega - \omega_{\sigma})d\omega_1d\omega_2, \quad (4)$$

where $\mathbf{P}_{\text{NL}}^{(2)}(\omega)$ is the nonlinear polarization producing the SESHG and $\mathbf{E}(\omega_1)$ and $\mathbf{E}(\omega_2)$ are the counterpropagating fundamental fields. Since only the power spectra $P(\omega_i)$ are known, we approximate $\mathbf{E}(\omega_i) \approx \sqrt{|P(\omega_i)|}$. The measured SESHG spectrum is clearly blueshifted, as expected from the observed distortion of the fundamental. The additional features in the measured SESHG spectrum result from the wavelength response of the distributed Bragg reflector.

In summary, we have presented data showing asymmetric spectral distortion of 240-fs pulses transmitted through a multilayer GaAs-Al_{0.9}Ga_{0.1}As SESHG waveguide. The distortion is consistent with the index changes caused by TPA-generated free carriers in the GaAs layers. We have measured the effective TPA coefficients for the waveguide to be $\beta^{\text{TM}} = 3$ cm/GW and $\beta^{\text{TE}} = 8$ cm/GW, and we have reproduced the measured spectra by a simulation using the experimentally measured parameters.

This work is supported in part by BellSouth, Corning, Nortel Networks, and the Georgia Research Alliance. T. Ulmer's e-mail address is gt0021e@prism.gatech.edu.

*Present address, Hewlett-Packard Singapore, 1150 Depot Road, Singapore.

References

1. K. A. Shore, X. Chen, and P. Blood, *Prog. Quantum Electron.* **20**, 181 (1996).
2. R. Normandin, S. Létourneau, F. Chatenoud, and R. L. Williams, *IEEE J. Quantum Electron.* **27**, 1520 (1991).
3. H. Dai, S. Janz, and R. Normandin, *Proc. SPIE* **1794**, 444 (1992).
4. D. Vakhshoori and S. Wang, *IEEE J. Lightwave Technol.* **9**, 906 (1991).
5. R. K. Tan, C. M. Verber, and A. J. SpringThorpe, *IEEE Photon. Technol. Lett.* **6**, 1228 (1994).
6. R. Normandin, R. L. Williams, and F. Chatenoud, *Electron. Lett.* **26**, 2088 (1990).
7. P. A. Ramos and E. Towe, *Opt. Commun.* **132**, 121 (1996).
8. J. S. Aitchison, D. C. Hutchings, J. U. Kang, G. I. Stegeman, and A. Villeneuve, *IEEE J. Quantum Electron.* **33**, 341 (1997).
9. N. Finlayson, E. M. Wright, and G. I. Stegeman, *IEEE J. Quantum Electron.* **26**, 770 (1990).
10. K. Hsia and C. D. Cantrell, *Proc. SPIE* **1497**, 166 (1991).
11. I. Androsch and P. Glas, *Opt. Commun.* **105**, 125 (1994).
12. B. R. Bennett, R. A. Soref, and J. A. Del Alamo, *IEEE J. Quantum Electron.* **26**, 113 (1990).
13. A. A. Said, M. Sheik-Bahae, D. J. Hagan, T. H. Wei, J. Wang, J. Young, and E. W. Van Stryland, *J. Opt. Soc. Am. B* **9**, 405 (1992).